The influence of rare-earth ions on the low-temperature thermoluminescence of $Bi_4Ge_3O_{12}$

2000 J. Phys.: Condens. Matter 12 2103

(http://iopscience.iop.org/0953-8984/12/9/314)

J. Phys.: Condens. Matter **12** (2000) 2103–2122. Printed in the UK PII: S0953-8984(00)08072-3

The influence of rare-earth ions on the low-temperature thermoluminescence of $Bi_4Ge_3O_{12}$

S G Raymond†‡ and P D Townsend†

† School of Engineering, Pevensey Building, University of Sussex, Brighton BN1 9QH, UK
‡ Department of Physics, Eastern University, Chenkalady, Sri Lanka

Received 23 September 1999, in final form 8 November 1999

Abstract. Low-temperature (20–290 K) thermoluminescence spectra of $Bi_4Ge_3O_{12}$ reveal a range of trapping levels, some of which are common to both undoped and doped material. The emission spectra for undoped and transition-metal-doped $Bi_4Ge_3O_{12}$ indicate that at low temperatures, intrinsic luminescence centres result in broad-band emission typical of signals from relaxed excitons or possibly excited bismuth ions. For material containing rare-earth ions, the signals are characteristic of the rare-earth dopants, even when the rare-earth ions are present in concentrations as low as 3 ppm. The temperatures of the glow peaks seen at ∼54, 105 and 141 K for undoped material are strongly modified by the rare-earth ions. The trapping and recombination sites, monitored by rare-earth emission, are intimately linked, probably within large complex structures. For these three glow peaks the peak temperature varies smoothly with the ionic radii of the rare-earth impurities. These movements are substantial, with changes of up to 50 K, as a function of the rare-earth radii. Of all the rare-earth ions, europium forms the most stable recombination centres. This is probably because the trivalent europium ion is similar in size to the host (bismuth) ion for which it substitutes. Tentative models for trapping sites and thermoluminescence mechanisms are proposed.

1. Introduction

Bismuth germanate ($Bi_4Ge_3O_{12}$) single crystals are used in a wide range of luminescence applications as well as optoelectronics (e.g. [1–6]). For each type of application there is an interest in the defect structures which exist within the crystal. However, a great deal remains unknown about the defect structures of this solid, particularly with regard to the production of luminescence. In principle the emission spectra recorded during thermoluminescence could provide an improved understanding of defect properties of the material, and certainly the high sensitivity of the technique is capable of resolving the influence of impurity ions on the signals from pure material. This article reports such thermoluminescence spectral measurements carried out on several undoped and doped $Bi_4Ge_3O_{12}$ single crystals.

Although in most applications $Bi_4Ge_3O_{12}$ scintillators are used at room temperature, increased luminescence sensitivity, and fundamental data on the modified lattice sites, may be obtained if the material is cooled to below room temperature [7]. Operation below room temperature is also required in some applications using $Bi_4Ge_3O_{12}$, such as in atmospheric studies [8].

Experimental information on the performance of $Bi_4Ge_3O_{12}$ crystals at temperatures below room temperature is very sparse. In particular, very little is known about the thermoluminescence emission spectra of undoped and doped $Bi_4Ge_3O_{12}$. In this article thermoluminescence spectral measurements made below room temperature are presented and discussed.

0953-8984/00/092103+20$30.00

An additional advantage of low-temperature thermoluminescence is that there are no problems of discriminating between thermoluminescence signals and black-body emission at the red end of the spectrum, as occurs in high-temperature thermoluminescence. The new data show some very clear trends in which the glow peak temperatures are sensitive to the ionic radii of rare-earth dopants. For $Bi_4Ge_3O_{12}$ this is a much larger variation than was reported for rare-earth-doped LaF_3 [9].

2. Experimental procedure

Low-temperature (20–290 K) thermoluminescence spectra were recorded using a high-sensitivity thermoluminescence spectrometer developed at the University of Sussex. The construction and operation of this apparatus has been described in detail by Luff and Townsend [10]. The nominally 'pure' (undoped), rare-earth-doped and transition-metal-doped $Bi_4Ge_3O_{12}$ samples used in this experiment were grown at the Shanghai Institute of Ceramics in the People's Republic of China by using the Bridgeman–Stockbarger technique. All samples were (100) cut. Table 1 lists the rare-earth (RE) and transition-metal (TM) doping concentrations of $Bi_4Ge_3O_{12}$ samples. In certain cases three ppm of europium were added to the melt to enhance the quality of the crystal. All samples were of 1 mm thickness.

Table 1. Dopant concentrations of $Bi_4Ge_3O_{12}$ samples.

Dopant	Doping level (wt% in melt)
Ce_2O_3	0.1
Nd_2O_3	0.4
Sm_2O_3	2.0
Eu_2O_3	0.3
Gd_2O_3	0.1
Tb_2O_3	2.0
Dy_2O_3	1.0
Ho_2O_3	1.0
Er_2O_3	1.0
Tm_2O_3	0.4
Cr_2O_3	0.02
MnO	0.02
NiO	0.02
CuO	0.02
WO_3	0.02
PbO	0.02

A Cryophysics model M22 cryostat was used in conjunction with a Lake Shore DRC-93C controller for the temperature ramping. Prior to heating, the samples were x-ray irradiated at dose rates of either 0.7 Gy min^{-1} or 20 Gy min^{-1} from a MCN-101 x-ray tube at 20 K. The thermoluminescence spectra were recorded at a rate of one per second and data were subsequently smoothed by using a spectral integration time of 3 s. The heating rate was 6 K min^{-1}. The spectrometers can record emission over the wavelength range from 200 to 800 nm. A pair of grating spectrometers, each with a position-sensitive (imaging photon detector) photomultiplier tube, were used for wavelength-multiplexed spectral analysis with photon-counting sensitivity. The gratings, one at each detector, disperse the signal across the relevant range i.e. 200–450 nm and 400–800 nm. All spectral data are corrected for the

wavelength dependence of the system. Entrance slits of 0.5 mm were used on the spectrometers giving approximately an 11 nm resolution over the whole wavelength range. A 400 nm cut-off filter was permanently inserted into the light path to the red detector to reduce the second-order diffraction of lower wavelengths into the first-order spectrum, but some signals beyond 780 nm include residual second-order effects and so are excluded in data shown here.

3. Results

The spectral changes with temperature are most readily visualized from the isometric plots, as for figure 1. Different viewing directions are chosen in the figures to reveal features which would otherwise be hidden. For more quantitative description of the data, some examples of contour maps and spectral slices at fixed temperatures are included in figures 2 and 3, respectively. The latter are transposed from wavelength data ($I(\lambda)\ \mathrm{d}(\lambda)$), as recorded, to the physically more meaningful energy plots ($I(E)\ \mathrm{d}E$). It is apparent from the thermoluminescence spectra of undoped $Bi_4Ge_3O_{12}$ (see figure 1) that the very-low-temperature glow peaks have a broad-blue/green-band luminescence. The spectrum closely resembles the radioluminescence spectra taken at 20 K where the luminescence band peaks around 480 nm. The emission spectra broaden and shift towards longer wavelength with increasing temperature. The broad bands extend variously from ∼400 to ∼650 nm below 100 K, or from ∼450 to ∼750 nm for glow peaks from 100 to 150 K. None of the earlier measurements [11, 12] revealed this type of spectral dependence with temperature.

The thermoluminescence emission spectra of $Bi_4Ge_3O_{12}$ doped only with transition metals broadly resemble the undoped spectra (see figure 1). When traces of europium were present in the crystal, at approximately a concentration of 3 ppm, the emission spectra of glow peaks between 100 and 200 K consisted of both intrinsic broad bands and Eu^{3+} characteristic lines. The thermoluminescence peaks above 200 K have only the Eu^{3+} characteristic lines. These measurements indicate that the thermoluminescence spectra have the sensitivity to respond to trace impurities of rare-earth ions at the ppm level.

An attempt was made to deconvolve the broad emission spectra of undoped and transition-metal-doped samples in terms of Gaussian energy bands. One temperature slice from each of the 20–50 K, 50–100 K and 100–150 K ranges was chosen for analysis. The peak positions analysed and the corresponding full widths at half-maximum are tabulated in table 2. Most of the slices in the highest temperature range of glow peaks were either too weak to be deconvolved, or had been replaced by Eu^{3+} characteristic lines. However, below 100 K the

Table 2. Gaussian band analysis of spectral slices taken from the isometric plots of undoped and transition-metal-doped $Bi_4Ge_3O_{12}$ samples.

	Peak E (eV)			Width ΔE (eV)		
Sample	20–50 K	50–100 K	100–150 K	20–50 K	50–100 K	100–150 K
BGO	2.54	2.59	2.19, 2.59	0.62	0.70	0.71, 0.71
BGO:Cr	2.47	2.50	—	0.62	0.69	—
BGO:Mn	2.43	2.45	—	0.61	0.68	—
BGO:Ni	2.52	2.64	—	0.67	0.73	—
BGO:Cu	2.47	2.50	2.50, 2.12	0.62	0.73	0.47, 0.47
BGO:W	2.50	2.59	—	0.66	0.73	—
BGO:Pb	2.50	2.57	—	0.64	0.69	—

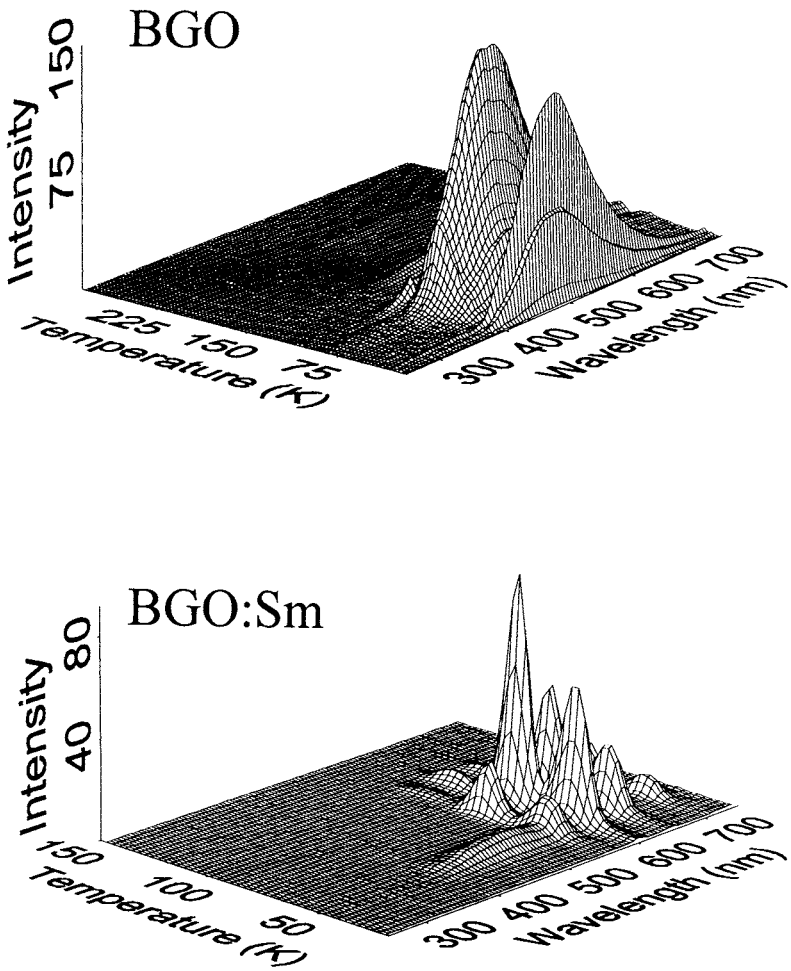

Figure 1. Some examples of thermoluminescence spectra of undoped, transition-metal- and rare-earth-doped $Bi_4Ge_3O_{12}$.

measured data are well described by a single emission band. There is a spread in the value of the peak position and the full width at half-maximum. In general the peak value slightly increases when it moves from the first to the second temperature range of glow peaks, even for the same sample.

Thermoluminescence emission spectra of the RE_2O_3-doped $Bi_4Ge_3O_{12}$ (see figures 1 and 2) reveal that they have a general pattern where the first few glow peaks (i.e. at very low temperature <100 K) have a composite emission from broad bands, and sometimes also show line features, but for the other glow peaks (at higher temperature >100 K) the spectra are predominantly in the form of narrow-line rare-earth emission. The broad-band emission is similar to that of the undoped $Bi_4Ge_3O_{12}$. A general observation from these thermoluminescence spectra of RE_2O_3-doped $Bi_4Ge_3O_{12}$ is that the luminescence character changes dramatically as soon as rare earths are introduced. Above 100 K, the broad-band signal which appeared in undoped $Bi_4Ge_3O_{12}$ is almost always suppressed, and replaced by some (but not all) of the internal transitions within the clearly identifiable energy level schemes

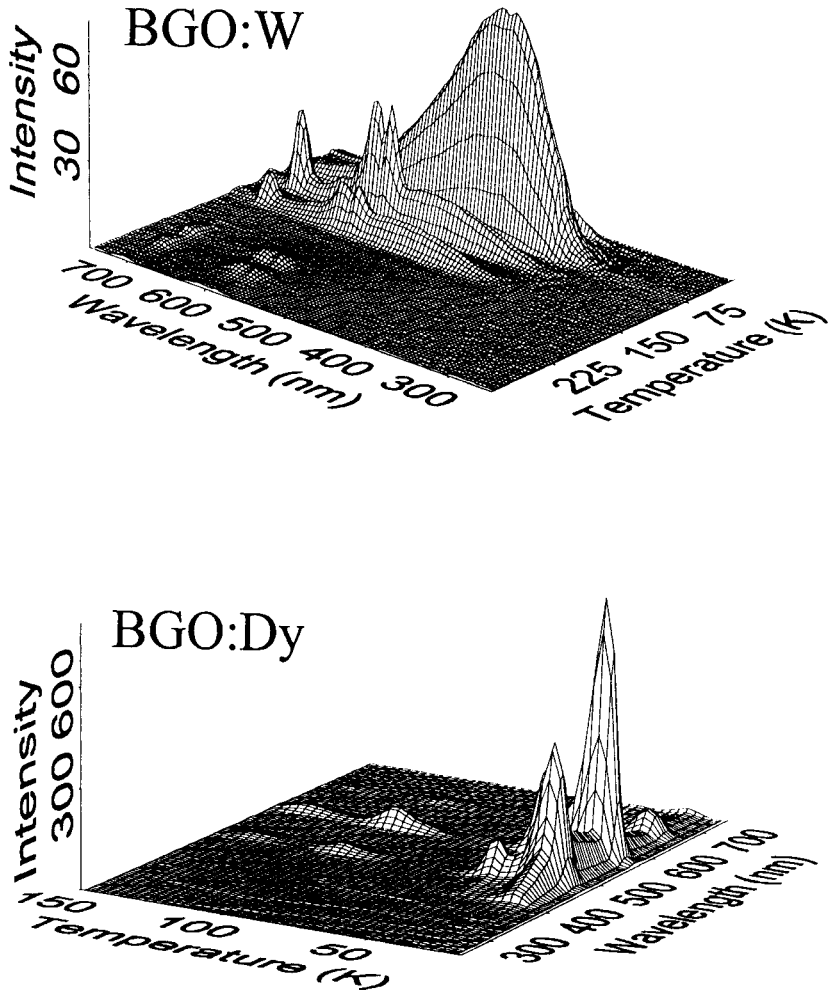

Figure 1. (Continued)

of the rare-earth ions. Below 100 K, the broad emission band can appear together with the emission spectra from the rare-earth ion.

Figure 2 displays examples of contour plots which underline this pattern of change from broad-band to line emission. Some examples of photon energy plots (see figure 3) also emphasize the shift in broad-band emission with temperature. Figures 4 and 5 present examples of normalized glow curves derived from the isometric data for the spectral regions at the wavelengths of the main emission lines. It is clear from these graphs that the line features and the intrinsic bands appear at nominally the same temperatures when both types of signal are apparent. However, it is equally clear that there are differences in peak temperature and glow curve shape between the samples. Indeed, the contour plots of the higher-temperature rare-earth signals of figure 2 differ dramatically and visual inspection of the figures does not immediately reveal common glow peaks. It is therefore essential to seek a pattern in the thermoluminescence responses and search for dopant-related trends.

A summary of the glow peak temperatures for the broad bands is given in table 3.

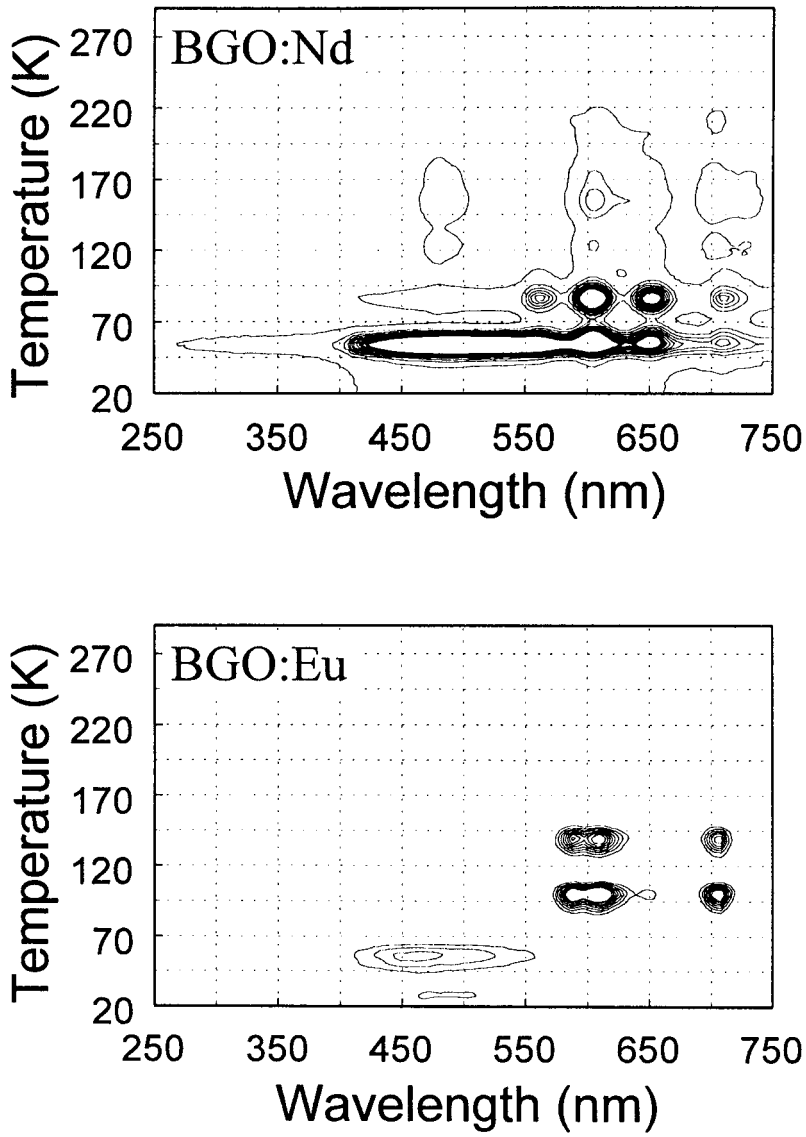

Figure 2. Contour maps of the thermoluminescence spectra of rare-earth-doped $Bi_4Ge_3O_{12}$.

4. Discussion

Since the thermoluminescence emission spectrum of undoped $Bi_4Ge_3O_{12}$ at very low temperatures is similar to the radioluminescence spectra of $Bi_4Ge_3O_{12}$, it might be associated with an intra-ionic transition of the Bi^{3+} ion, since Weber and Monchamp [7] interpreted this peak to arise from the $^3P_1 \longrightarrow {}^1S_0$ transition of the filled-shell (mercury-like) Bi^{3+} cation. So one possibility is that during the temperature ramping (at very low temperatures <100 K) the luminescence takes place at Bi^{3+} ions. This explanation is only partially successful since, as shown in figure 1, there are at least two main broad bands for undoped material which occur

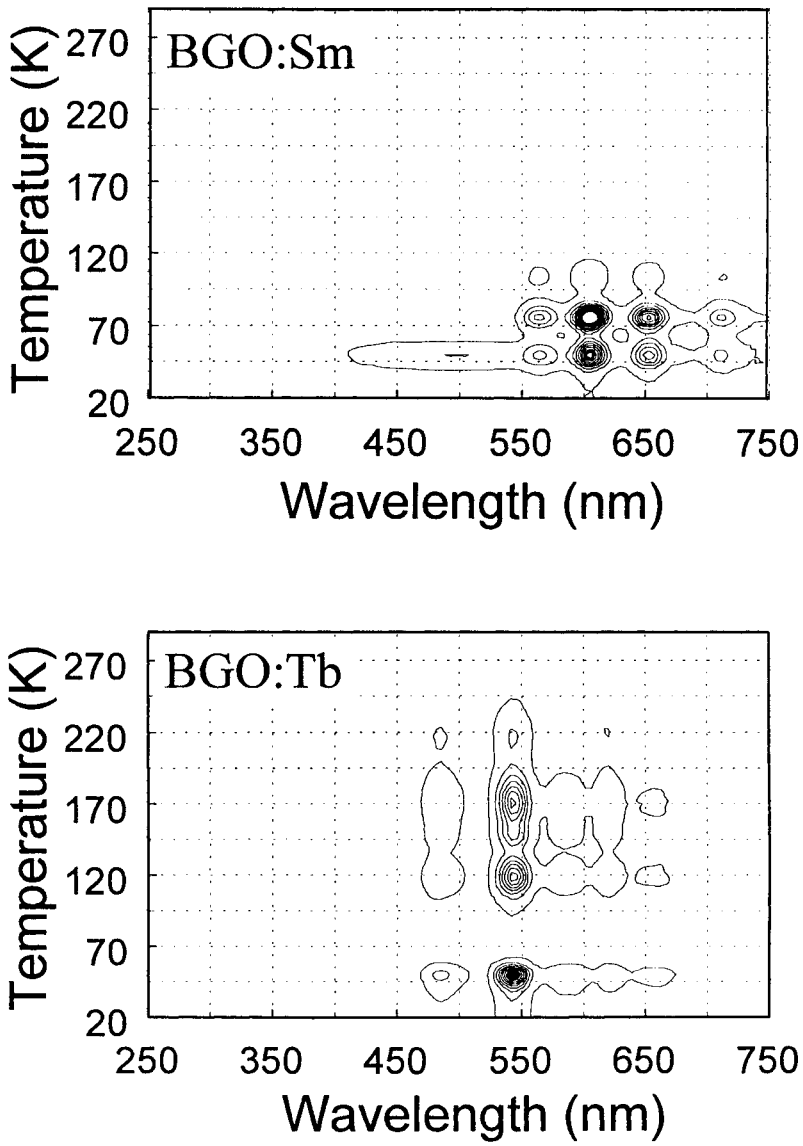

Figure 2. (Continued)

in different temperature regimes. Further, as listed in table 2, the peak positions vary between 2.43 and 2.64 eV when the material is doped with metal ions. Figure 6 shows the spectra for undoped $Bi_4Ge_3O_{12}$ in which the change in peak position, or combination of bands, is clearly apparent. Note that there are at least two glow peaks which are predominantly at 2.43 and two at 2.64 eV. Since the $Bi_4Ge_3O_{12}$ lattice has two non-equivalent oxygen sites, the pairs of glow peaks may therefore result from variants of basic defect types. Alternative models, such as decay of relaxed excitons in the presence of intrinsic or impurity defects, may however be preferable, as will be mentioned later.

At higher temperatures different luminescence centres become active. Note in particular

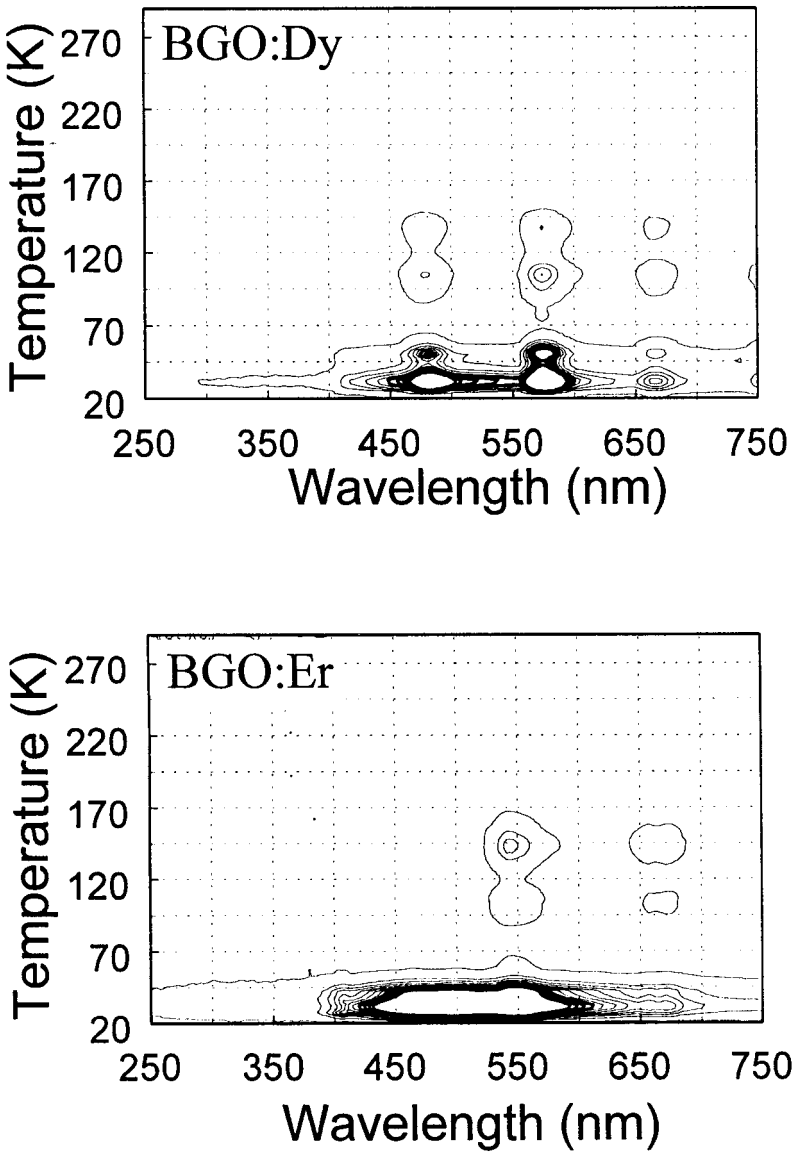

Figure 2. (Continued)

that although the band gap of $Bi_4Ge_3O_{12}$ would transmit signals in the UV down to at least 300 nm, there are only very weak signals in the broad-band spectra in the UV region. In general the broad-band thermoluminescence signals extend from ∼400 nm to beyond 750 nm, with main component peaks near 480 or 550 nm; see figure 6. Similarly, the line spectra are limited to this same long-wavelength region, even though in other materials, such as $CaSO_4$, the thermoluminescence activations by rare-earth dopants of Ce, Gd or Tm all emit in the 280 to 400 nm region where $Bi_4Ge_3O_{12}$ is transparent.

Low-temperature x-ray-induced optical measurements carried out by Zaldo and Moya [13, 14] indicated that, on heating the $Bi_4Ge_3O_{12}$ sample after x-ray irradiation at low

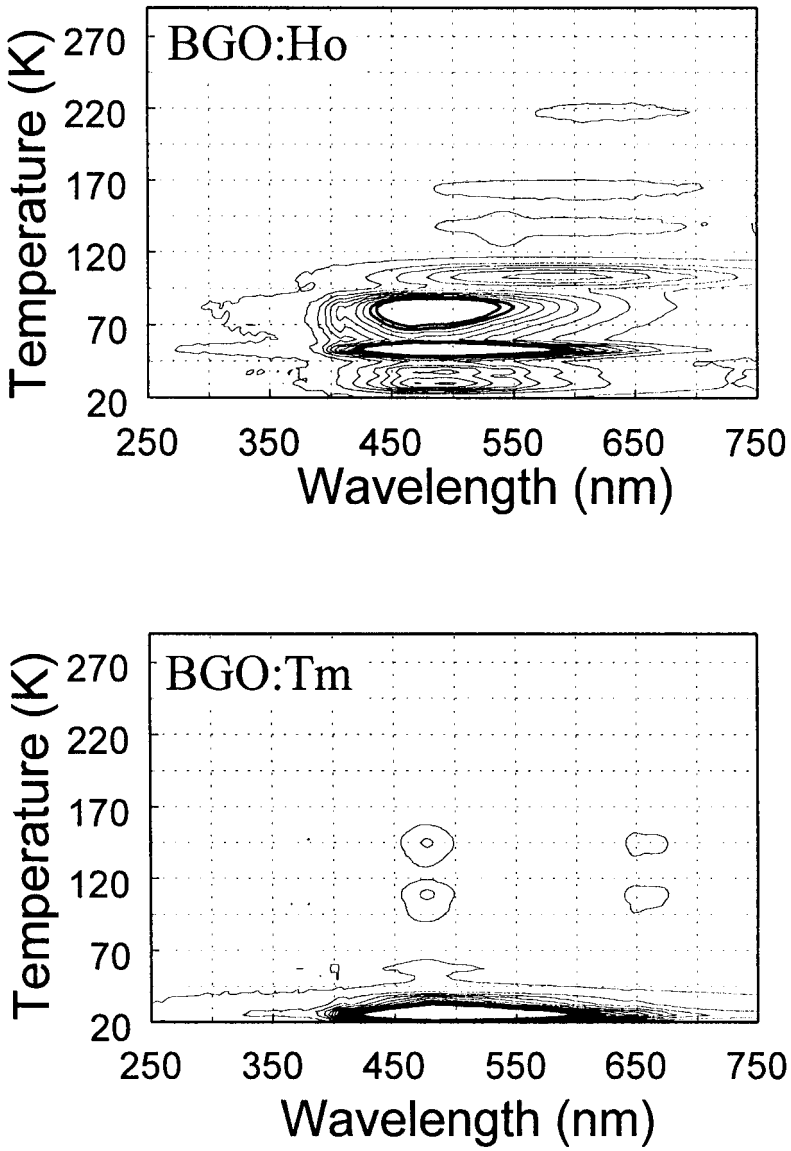

Figure 2. (Continued)

temperature, a broad intense optical absorption increased in the visible and ultraviolet regions. For $Bi_{12}GeO_{20}$ [15] and other oxides [16, 17] it is often suggested that holes trapped in the oxygen sublattice are responsible for the broad optical absorption bands observed after exposure to ionizing irradiation. So Zaldo and Moya [13, 14] assumed that similar types of absorption centre were present in $Bi_4Ge_3O_{12}$. It therefore follows that the broad thermoluminescence emission might come from related defects such as holes trapped in the oxygen sublattice. It is less clear whether the light is produced by hole release or by electrons moving to the hole sites during the thermoluminescence. According to Zaldo and Moya [13, 14], the most likely primary defects, created at low temperatures in $Bi_4Ge_3O_{12}$ by x-rays, are holes trapped

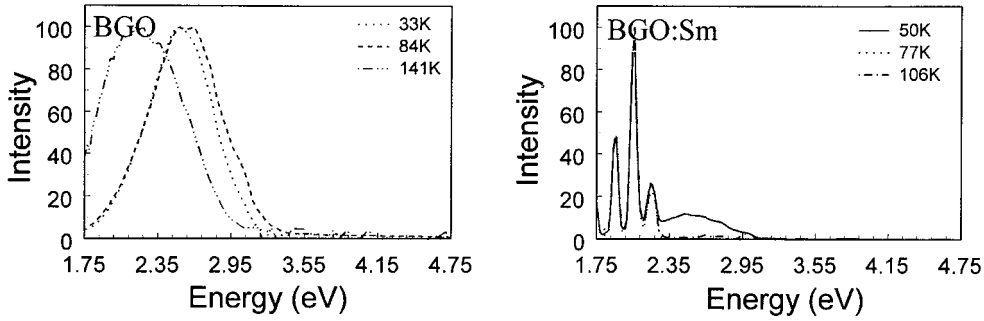

Figure 3. Some examples of normalized spectral slices at fixed temperatures.

Table 3. Thermoluminescence glow peak temperatures of undoped, transition-metal-doped or rare-earth-doped $Bi_4Ge_3O_{12}$ below room temperature when the emission is in the form of broad bands.

Sample	Glow peak temperatures (K)
Undoped	28, 33, 45, 54, 84, 105, 141
BGO:Cr	28, 36, 69, 106, 142
BGO:Mn	25, 34, 40, 54, 66
BGO:Ni	25, 37, 42, 58, 73, 108, 147, 169
BGO:Cu	24, 40, 51, 78, 109, 121, 145
BGO:W	30, 71, 101, 135
BGO:Pb	27, 31, 41, 61, 78, 112
BGO:Ce	28, 42, 67
BGO:Nd	55
BGO:Sm	50
BGO:Eu	35, 62
BGO:Gd	39, 77, 113, 152
BGO:Tb	—
BGO:Dy	31, 51
BGO:Ho	30, 40, 54, 82, 103, 139, 166
BGO:Er	32, 41
BGO:Tm	24, 35

on germanium ions or in cation vacancies. On raising the temperature, these trapped holes become unstable and are re-trapped in the oxygen sublattice. These defects, known as 'small-polaron' centres, give rise to the optical absorption of $Bi_4Ge_3O_{12}$ when the sample temperature is increased after x-ray irradiation at very low temperatures.

Simultaneously, the electrons excited, or released, by the low-temperature x-ray irradiation can be trapped by various types of electron trap (cation sites, oxygen vacancies etc) which are present in the crystal. It is assumed that some of the Bi^{3+} ions can reduce to Bi^{2+} by capturing electrons. When the temperature is raised after irradiation, holes trapped at cation sites are thermally released and become mobile. These holes can either be re-trapped in the oxygen sublattice, or recombine with Bi^{2+} and produce Bi^{3+} in excited energy states. De-excitation of these ions could yield luminescence, as summarized in the following way for the

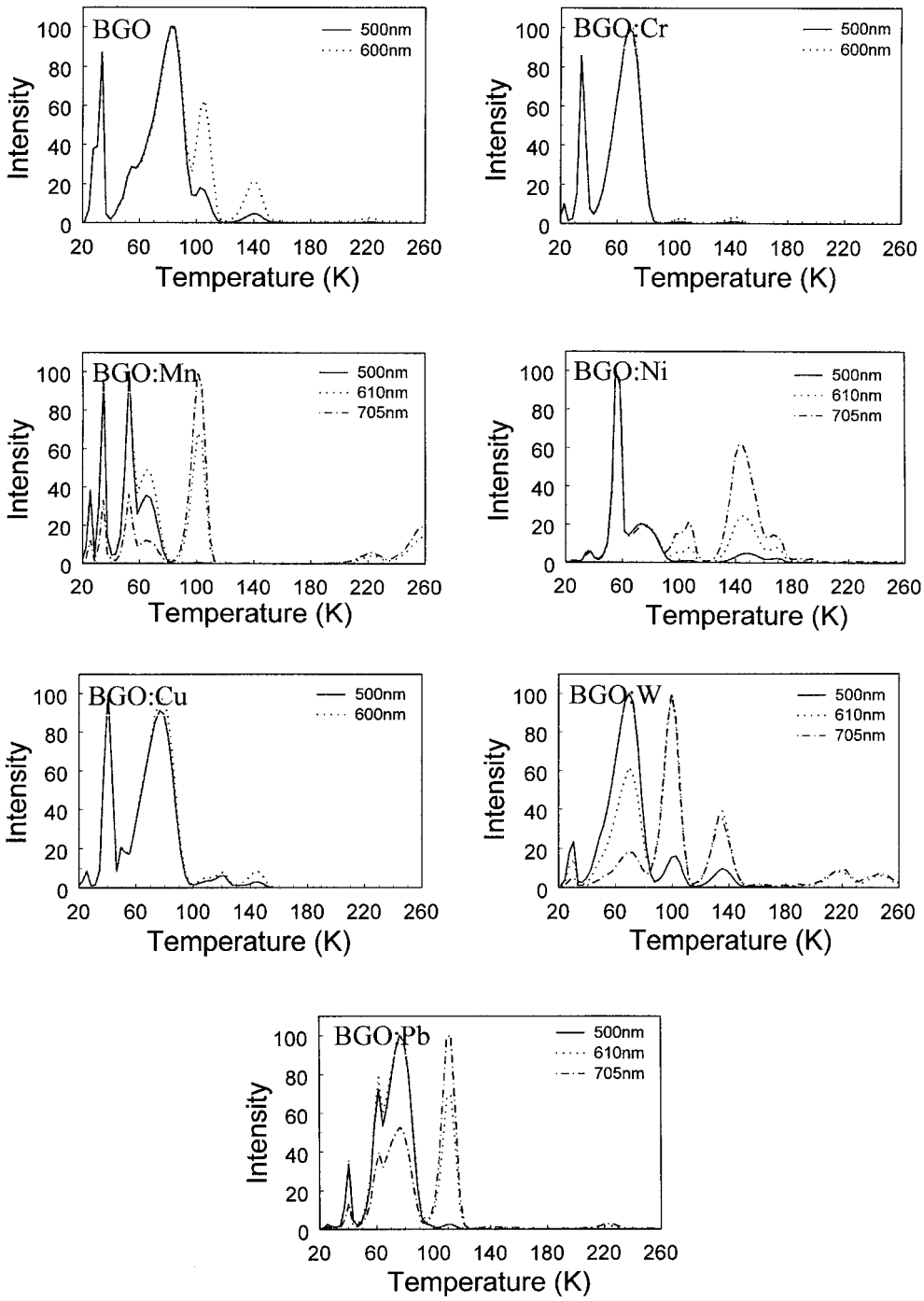

Figure 4. Normalized thermoluminescence glow curves of undoped and transition-metal-doped $Bi_4Ge_3O_{12}$.

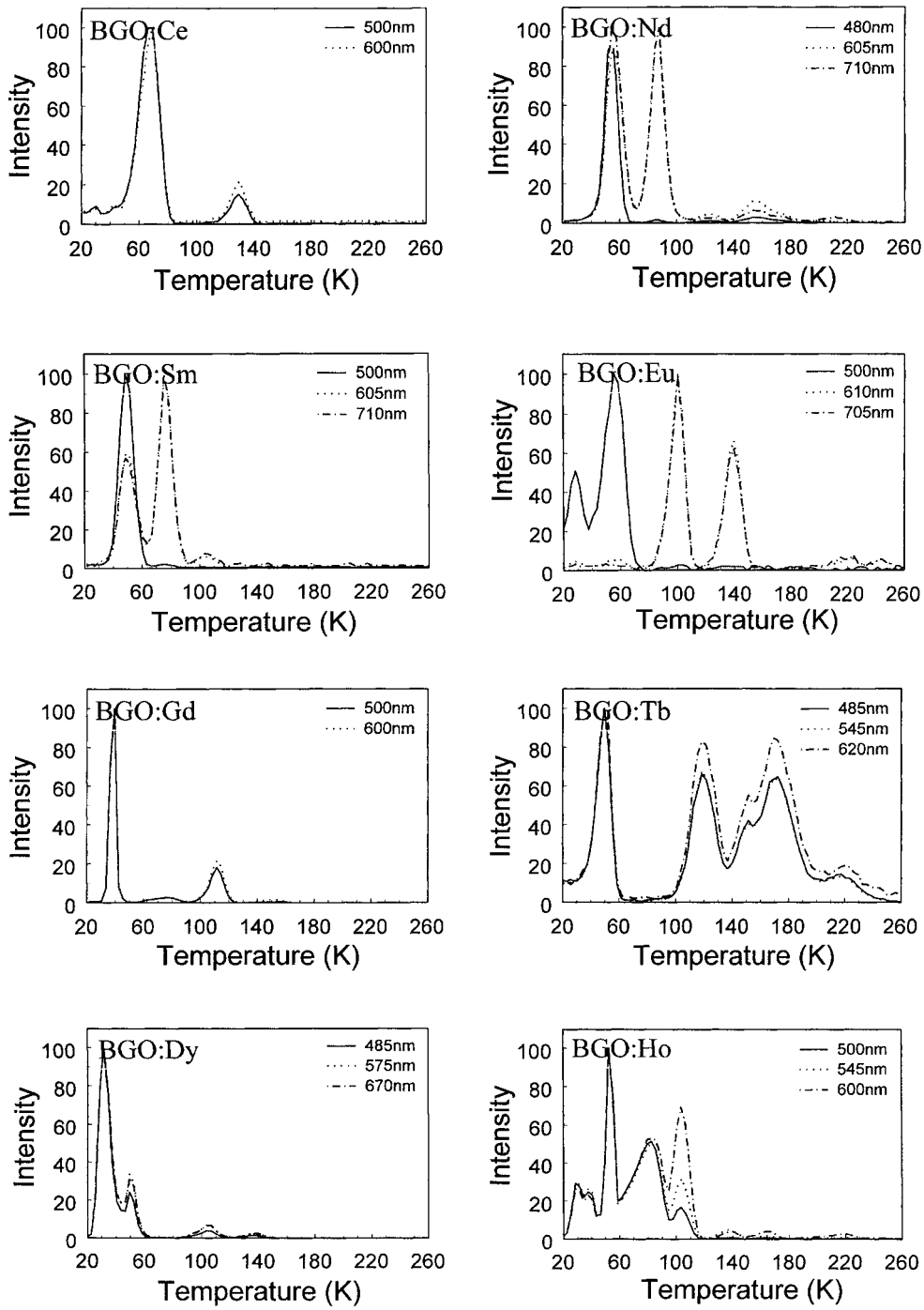

Figure 5. Normalized thermoluminescence glow curves of rare-earth-doped $Bi_4Ge_3O_{12}$.

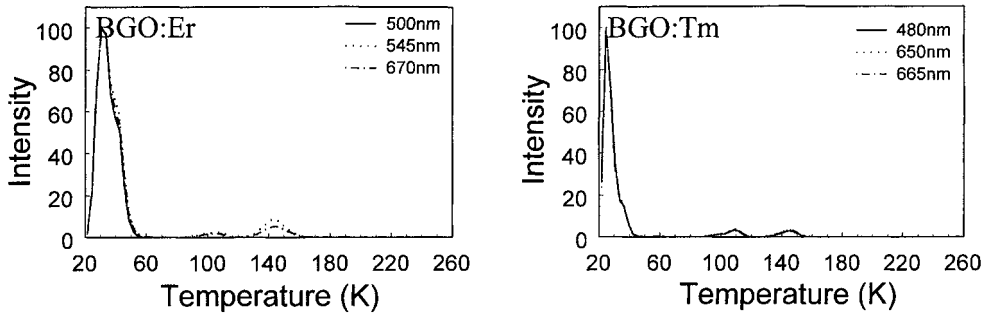

Figure 5. (Continued)

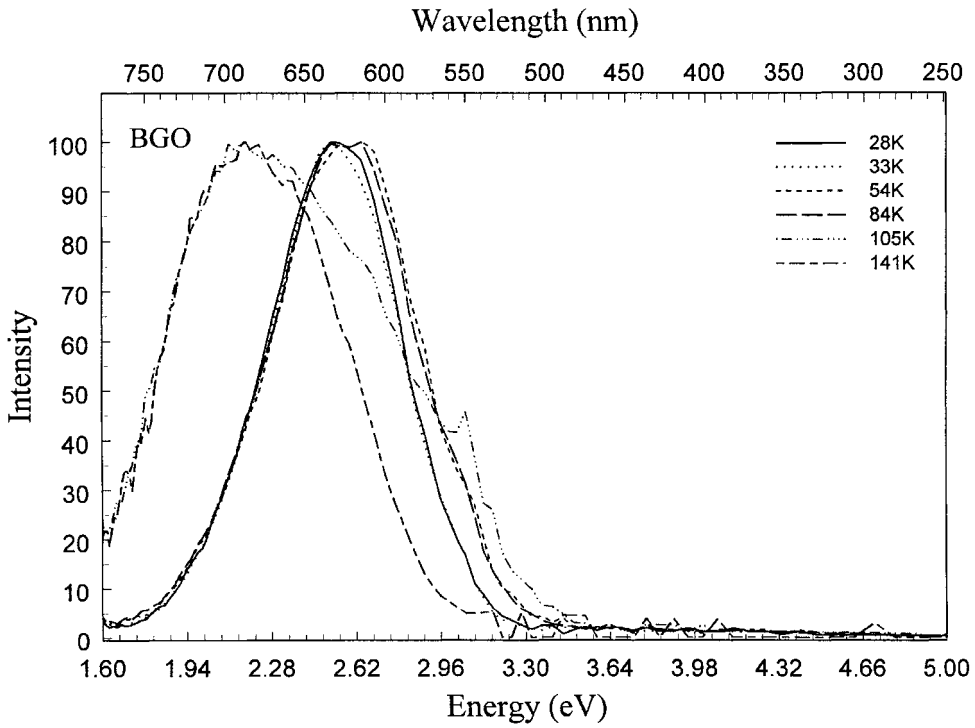

Figure 6. Broad-band emission spectra of undoped $Bi_4Ge_3O_{12}$ at low temperatures.

thermoluminescence processes below 100 K:

$$Bi^{3+} \longrightarrow Bi^{2+} + \text{hole centre (irradiation)}$$
$$\text{released hole} + Bi^{2+} \longrightarrow (Bi^{3+})^* \text{ (heating)}$$
$$(Bi^{3+})^* \longrightarrow Bi^{3+} + h\nu.$$

Moreover, when the temperature is raised above 100 K the electrons trapped in various traps can be released by thermal excitation and become mobile. Consequently, these electrons have the possibility of recombining with the holes trapped in the oxygen sublattice and hence would also produce broad-band luminescence.

According to the thermoluminescence model described above, the traps responsible for the glow peaks below 100 K are hole traps, while the others are electron traps. Possible intrinsic hole traps are germanium ions and cationic (bismuth or germanium) vacancies [13, 14]. In $Bi_4Ge_3O_{12}$ crystals, interstitial ions are unlikely because of the lack of space in the lattice. The O^{2-} ion is large (1.4 Å) and deformable. It tends to fill all the space between the Bi^{3+} and the Ge^{4+} ions. So it could be suggested that extrinsic defects in the crystal are substitutional. Further, particle-induced x-ray analysis of doped and undoped $Bi_4Ge_3O_{12}$ samples shows that these crystals contain a few ppm of iron and chromium. So these ions also may either form a hole trap or an electron trap depending on which host ion they are replacing. In addition to these defects, disruptions in the oxygen and germanium sublattices can create electron traps.

Such models are highly speculative, not least because for metal-doped material nominally the same broad-band emissions are observed. Table 2 indicated that there are specific shifts in band positions with dopant but no systematic pattern is obvious. As shown by table 4 it is equally unclear where in the lattice the various transition-metal ions are accommodated, since they differ considerably in valence and ionic size from both the Bi and Ge ions of the host.

Table 4. Ionic radii of metals [32]. Values for Bi^{3+} and Ge^{4+} in $Bi_4Ge_3O_{12}$ are indicated in bold face.

		Radius for different charge states (Å)						
Metal	Atomic number	+1	+2	+3	+4	+5	+6	+7
Cr	24	0.81	0.89	0.63	—	—	0.52	—
Mn	25	—	0.80	0.66	0.60	—	—	0.46
Fe	26	—	0.74	0.64	—	—	—	—
Ni	28	—	0.69	—	—	—	—	—
Cu	29	0.96	0.72	—	—	—	—	—
Ge	32	—	0.73	—	**0.53**	—	—	—
W	74	—	—	—	0.70	0.62	—	—
Pb	82	—	1.20	—	0.84	—	—	—
Bi	83	0.98	—	**0.96**	—	0.74	—	—

Above about 60 K, RE_2O_3-doped $Bi_4Ge_3O_{12}$ samples show the narrow emission bands characteristic of the internal transitions of the rare-earth 4f shell, which are relatively insensitive to the crystal field of the host, or the local ionic environment. Comparison with the energy level diagrams of RE^{3+} ions in $LaCl_3$ [18] identifies most of the observed line spectra obtained during the thermoluminescence of RE_2O_3-doped $Bi_4Ge_3O_{12}$. Table 5 lists the probable transitions for the narrow emission bands observed during the thermoluminescence of RE_2O_3-doped $Bi_4Ge_3O_{12}$. Note however that many potential lines are absent, particularly from all the higher-energy states above about 3 eV (i.e. wavelengths below 400 nm). Lines may also be quenched for high dopant concentrations (as for Nd in CaF_2 [19]).

It is assumed that the rare-earth ions substitute onto the Bi^{3+} sites, since they are trivalent and so require no charge compensation. Further, they are relatively similar in ionic radii to the Bi^{3+} ion and thus introduce relatively small amounts of lattice distortion. Accommodation of the rare-earth ions does not however indicate how they participate in the luminescence process. Alternatives could be that during irradiation they convert to a new valence state (2+ or 4+) and emit during return to the normal state, or that they always remain in the 3+ state but become excited and emit following a resonant energy transfer from the host. Variants of these models are for the rare-earth ions to be in isolation or to form part of large defect complexes. The most obvious difference between bulk and complex behaviour is that the trapping sites will be influenced by the rare-earth ion in the complex, and so this will alter the charge trapping energy

Table 5. Suggested transitions between RE^{3+} energy levels.

Wavelength (nm)	Assignment ($^{S}L_{J}$)
Nd_2O_3-doped $Bi_4Ge_3O_{12}$	
480	$^4G_{9/2} \longrightarrow {}^4I_{9/2}$
563	$^4G_{9/2} \longrightarrow {}^4I_{13/2}$
604	$^4G_{9/2} \longrightarrow {}^4I_{15/2}$
650	$^4G_{7/2} \longrightarrow {}^4I_{13/2}$
708	$^2G_{7/2} \longrightarrow {}^4I_{13/2}$
Sm_2O_3-doped $Bi_4Ge_3O_{12}$	
566	$^4G_{5/2} \longrightarrow {}^6H_{5/2}$
604	$^4G_{5/2} \longrightarrow {}^6H_{7/2}$
654	$^4G_{5/2} \longrightarrow {}^6H_{9/2}$
713	$^4G_{5/2} \longrightarrow {}^6H_{11/2}$
Eu_2O_3-doped $Bi_4Ge_3O_{12}$	
590	$^5D_0 \longrightarrow {}^7F_1$
610	$^5D_0 \longrightarrow {}^7F_2$
650	$^5D_0 \longrightarrow {}^7F_4$
705	$^5D_0 \longrightarrow {}^7F_5$
745	$^5D_0 \longrightarrow {}^7F_6$
Tb_2O_3-doped $Bi_4Ge_3O_{12}$	
485	$^5D_4 \longrightarrow {}^7F_6$
543	$^5D_4 \longrightarrow {}^7F_5$
585, 594	$^5D_4 \longrightarrow {}^7F_4$
621	$^5D_4 \longrightarrow {}^7F_3$
658	$^5D_4 \longrightarrow {}^7F_2$
Dy_2O_3-doped $Bi_4Ge_3O_{12}$	
484	$^4F_{9/2} \longrightarrow {}^6H_{15/2}$
575	$^4F_{9/2} \longrightarrow {}^6H_{13/2}$
667	$^4F_{9/2} \longrightarrow {}^6F_{11/2}$
759	$^4F_{9/2} \longrightarrow {}^6F_{9/2}$
Ho_2O_3-doped $Bi_4Ge_3O_{12}$	
543	$^5S_2 \longrightarrow {}^5I_8$
Er_2O_3-doped $Bi_4Ge_3O_{12}$	
544	$^4S_{3/2} \longrightarrow {}^4I_{15/2}$
658, 672	$^4F_{9/2} \longrightarrow {}^4I_{15/2}$
Tm_2O_3-doped $Bi_4Ge_3O_{12}$	
479	$^1G_4 \longrightarrow {}^3H_6$, $^3P_0 \longrightarrow {}^3F_2$
650, 663	$^1G_4 \longrightarrow {}^3H_4$
791	$^1G_4 \longrightarrow {}^3H_5$

as a function of the rare-earth ion. Hence, the glow peak temperature for equivalent defects will vary as a function of the rare-earth ion. For independent trapping and recombination sites

the glow peak temperatures will be insensitive to the rare earth which is used. The present data are valuable both for deciding between changes in the rare-earth valence state and in detecting the possibility of defect complexes which link the rare earth to a trapping site.

If during irradiation the RE^{3+} ions convert to RE^{2+} states (by gaining an electron), then during the thermoluminescence heating stage, the rare-earth ions are re-converted to the trivalent excited state and emit photons. But this process seems unlikely since there would also be a high probability that energy would be transferred into the RE^{2+} state. However, there is no spectral evidence for 2+ emission and for some rare-earth ions, such as Eu, this would be unmistakable. Suppression of RE^{2+} emission might also occur if the states were unfavourably positioned relative to the $Bi_4Ge_3O_{12}$ energy gap. Physically, however, RE^{2+} formation seems an unlikely situation for a long-term charge storage as the volume of a RE^{2+} ion is some 60% greater than for the equivalent RE^{3+} state. Such lattice distortions would be difficult to accommodate.

Alternatively, if the holes released during the low-temperature ramp were re-trapped at RE^{3+} sites, rather than in the oxygen sublattice, as in undoped $Bi_4Ge_3O_{12}$, then this hole trapping would convert RE^{3+} to RE^{4+} ions. During the thermoluminescence heating stage, the electrons released from various traps could recombine with the holes trapped at rare-earth ions and emit the characteristic spectra of the impurity. The weakness of this model is that high energy levels of the trivalent ion should be excited and so a full wavelength range of emission spectra would be detected. This is certainly not the case for Ce, Gd or Tm dopants.

The totally different possibility, which was already mentioned, is that electron and hole recombination taking place at normal lattice sites forms exciton-like states (albeit with an enhanced recombination probability for sites near imperfections). For $Bi_4Ge_3O_{12}$ the band gap is at about 280 nm in terms of wavelength, which sets an upper energy limit. However, in most oxides the exciton relaxes before decay [20–22] and so gives broad-band emission at longer wavelengths. The exciton is relatively insensitive to the dielectric constant of the host, so typically this relaxed exciton decay is from 380 to 550 nm, and is shifted in the same host in the presence of impurities. Resonant energy transfer from this decay route can thus only stimulate transitions with an upper energy defined by this intrinsic relaxed exciton decay. Hence there is an obvious correlation explaining why the intrinsic broad-band emissions at the lowest temperature are primarily at wavelengths longer than ∼400 nm (relaxed excitons) and the higher-energy tail is very weak (direct processes). Further, this defines the limit of wavelengths from the rare-earth dopants. In particular, as observed here, it inhibits the Ce or Gd transitions, or the short wavelength signals from Tm.

Comparison with data for other materials gives a direct analogy with the present data as the thermoluminescence results from $CaSO_4$:Tm, [23, 24], $CaSO_4$:Ce [25], $CaSO_4$:Dy [26], CaF_2:Nd [19] and CaF_2:Gd [33] show in each case that the full range of higher-energy states are strongly emitted. However, these are wider-band-gap materials and the relaxed exciton energies are generated at wavelengths between ∼300 and 400 nm. The current data are thus consistent with a similar mechanism of energy transfer of relaxed exciton decay energy to excite a RE^{3+} ion, with an upper energy limit set by the energy of the exciton. For the $Bi_4Ge_3O_{12}$ this limits the wavelengths to those longer than ∼400 nm.

The second question to address is that of whether the rare-earth ion and the trapping sites are independent and/or if the rare-earth ions are within large complex structures. Literature examples of rare-earth dopants in for example the alkaline-earth fluorides [20, 21] strongly suggest that several rare-earth ions, together with other intrinsic defects, form a large assembly [27]. In $CaSO_4$ with say Tm and Dy the glow peaks show characteristic rare-earth emission lines but they are displaced by about 8 °C; in magnesium borate the differences are larger and up to 30 degrees [24]. For LaF_3 [9] the 128 K peak is shifted smoothly by up to 14

degrees as a function of the dopant rare-earth ionic radius, and also appears to have a change in configuration of the bonding. A more tentative interpretation of recent thermoluminescence data for rare-earth-doped synthetic zircon [28] suggests a glow peak shift which scales in temperature with ionic radius of the rare earth, but the temperature movement spans almost 200 degrees. In all these examples the argument is that if the rare-earth recombination site influences the glow peak temperature, then the rare earth and the trapping component are intimately linked, probably within the same complex.

For $Bi_4Ge_3O_{12}$, earlier high-temperature thermoluminescence data showed a small shift [29] of peak temperature which scaled smoothly for rare-earth ions smaller than Bi. In that case the argument was that the rare earth was coupled to a simple defect, probably a vacancy. Assuming that the activation energy was unaltered, the changes in rare-earth mass were sufficient to influence the vibrational frequency of the complex and so shift the glow peak through the observed range of less than 10 degrees. In the new low-temperature data presented here it is necessary to consider two temperature ranges.

Below about 100 K, where there are broad-band emissions from intrinsic processes, such as hole trapping and then relaxed exciton-type radiative decay, the rare-earth ions are directly in competition with the intrinsic processes. Both broad bands and rare-earth line features coexist at nominally the same temperature, independent of the rare-earth dopant. In this situation one assumes that the excitons are formed and then relax and/or migrate to interact with intrinsic or impurity sites. Emission is then either broad-band intrinsic or rare-earth line in character, resulting from resonant energy transfer. However, the original trapping sites and the rare-earth recombination sites are independent and so there is negligible influence of the rare-earth ions on the binding energy of the charge traps. Impurities do however influence the precise position of the spectra (see table 2). Note that hole centres are likely to be stable and dominant in these low-temperature regions, whereas fewer hole traps are stable at higher temperatures in $Bi_4Ge_3O_{12}$, and instead electron traps are dominant (e.g. [13, 14]). This is the same pattern as is observed for most insulating materials [20, 21].

Above about 60 K a totally different pattern starts to emerge in which the rare-earth ions do not generally emit at the same temperature. In order to try to seek size-related trends in the data the main glow peak temperatures are plotted in figure 7 as a function of rare-earth ionic radii. The intrinsic data from undoped material fit these plots at the points indicated by the Bi^{3+} ionic radius. The points with the lines shown in the figure offer a pattern for three strong glow peaks which link with the minimum temperatures for the undoped material, and higher values in the strained lattice. The smallest temperature shifts occur for Eu, which is close in size, but smaller than the Bi ion (note that it is used as a crystal growth stabilizer). Divergence from the 'perfect' fit into the lattice introduces progressively larger strains and distortions of the local atomic arrangements near the impurity, and consequently changes in the glow peak temperatures. In each case this implies that the trapping defects are very strongly coupled to the rare-earth recombination sites and there is energy transfer within the complexes. The data do not clearly indicate whether only one rare-earth ion exists per complex, or whether several impurity ions coalesce into the same package. For the relatively small size mismatch, and a perfect charge situation, isolated rare-earth ions are a reasonable first assumption, but certainly pairing or clustering might favour reduction of lattice strain energy. Note that in the well documented literature on ruby the Cr^{3+} distortion caused by substitution of an oversize ion onto the Al^{3+} site leads to adjacent pairs of impurity ions in order to minimize strain. In that case the ionic radii of Cr^{3+} and Al^{3+} are approximately 0.063 and 0.054 nm respectively [21]. Related data on both luminescence rare-earth line broadening [30] and surface second-harmonic generation [31] of rare-earth-doped $Bi_4Ge_3O_{12}$ follow very similar patterns to that shown in figure 7, with a minimum effect for Eu and Sm ions which are most easily accommodated into the lattice.

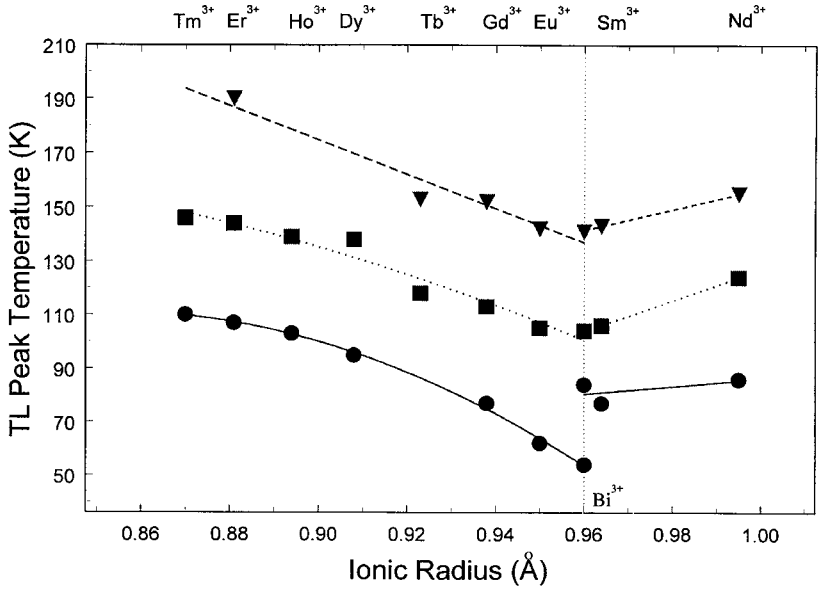

Figure 7. A plot of the glow peak temperatures of rare-earth-doped $Bi_4Ge_3O_{12}$ as a function of the rare-earth ionic radii [32].

The analysis presented above strongly favours a simple predictable trend of peak shift with dopant rare-earth size. However, one test of the model is to consider codoped material, since in the simplest situation, each dopant might behave independently. For $Bi_4Ge_3O_{12}$ this does not appear to be the case. In a sample heavily doped with Nd and Er (at 0.4%) and Eu at 3 ppm, all three ions emit simultaneously with the intrinsic broad bands at 100 K, but at progressively higher temperatures the emission is via the Eu, and the glow peak temperatures are mostly determined by those of Eu. This codoped response differs from that seen for calcium sulphate where the Dy and Tm lines are clearly separated in temperature, or for LaF_3 where codoping introduces new peak temperatures intermediate between those of the separate ions (i.e. consistent with several rare-earth ions per complex site).

The data presented here reveal clear trends in glow peak temperature as a function of rare-earth dopant. The lattice distortions that they introduce move the undoped peak temperature to higher values. Whilst trends do not reveal the defect model, the scale of the glow peak shifts is very large (e.g. from 54 to 110 K) which indicates not only a major lattice defect distortion but also an intimate coupling between the trapping and recombination site. The inference is that the defect complex involves several lattice sites.

5. Conclusions

Measurements of thermoluminescence emission spectra reveal common features of intrinsic broad-band emission for low-temperature glow peaks which appear at similar temperatures for undoped and transition-metal-doped $Bi_4Ge_3O_{12}$. By contrast the high-temperature glow peaks obtained with rare-earth dopants vary in temperature according to the size of the rare-earth ion. Models of large complex defect sites are required to explain such behaviour.

Acknowledgment

SGR is grateful to the Royal Society for a Fellowship.

References

[1] Johnson T F and Ballman A A 1969 Coherent emission from rare earth ions in electro-optic crystals *J. Appl. Phys.* **40** 297–302
[2] Nestor O H and Huang C Y 1975 Bismuth germanate: a high-*Z* gamma-ray and charged particle detector *IEEE Trans. Nucl. Sci.* **22** 68–71
[3] Moya E, Contreras L and Zaldo C 1988 $Bi_4Ge_3O_{12}$:Cr: a new photorefractive material *J. Opt. Soc. Am.* B **8** 1737–42
[4] Mahdavi S M, Chandler P J and Townsend P D 1989 Formation of planar waveguides in bismuth germanate by He^+ ion implantation *J. Phys. D: Appl. Phys.* **22** 1354–7
[5] Field S J, Hanna D C, Large A C, Shepherd D P, Tropper A C, Chandler P J, Townsend P D and Zhang L 1991 Ion-implanted crystal waveguide lasers *Opt. Soc. Am. Proc. Adv. Solid State Lasers* **10** 353–7
[6] Brockelsby W S, Field S J, Hanna D C, Large A C, Lincoln J R, Shepherd D P, Tropper A C, Chandler P J, Townsend P D, Zhang L, Feng X and Hu Q 1992 Optically written waveguides in ion implanted $Bi_4Ge_3O_{12}$ *J. Opt. Mater.* **1** 177–84
[7] Weber M J and Monchamp R R 1973 Luminescence of $Bi_4Ge_3O_{12}$: spectral and decay properties *J. Appl. Phys.* **44** 5495–9
[8] Rester A C, Coldwell R L, Trombka J I, Starr R, Eichhorn G and Lasche G P 1990 Performance of bismuth germanate active shielding on a balloon flight over Antarctica *IEEE Trans. Nucl. Sci.* **37** 559–65
[9] Yang B, Townsend P D and Rowlands A P 1998 Low-temperature thermoluminescence spectra of rare-earth-doped lanthanum fluoride *Phys. Rev.* B **57** 178–88
[10] Luff B J and Townsend P D 1993 High sensitivity thermoluminescence spectrometer *Meas. Sci. Technol.* **4** 65–71
[11] Diéguez E, Arizmendi L and Cabrera J M 1985 X-ray induced luminescence, photoluminescence and thermoluminescence of $Bi_4Ge_3O_{12}$ *J. Phys. C: Solid State Phys.* **18** 4777–83
[12] Gusev V A and Petrov S A 1989 Local trap centres in $Bi_4Ge_3O_{12}$ crystals *Z. Prikl. Spektrosk.* **50** 627–31
[13] Zaldo C and Moya E 1993 Low-temperature x-ray-induced optical properties of $Bi_4Ge_3O_{12}$ scintillators *J. Phys.: Condens. Matter* **5** 4935–44
[14] Zaldo C and Moya E 1993 Optical properties of $Bi_4Ge_3O_{12}$ scintillators after low temperature x-ray irradiation *Defects in Insulating Materials* ed O Kanert and J M Spaeth (Singapore: World Scientific) pp 1139–41
[15] Moya E and Zaldo C 1992 X-ray-induced defects in $Bi_{12}GeO_{20}$ single crystals *J. Phys.: Condens. Matter* **4** L287–91
[16] Schirmer O F, Koidl P and Reik H G 1974 Bound small polaron optical absorption in V^--type centres in MgO *Phys. Status Solidi* b **62** 385–91
[17] Schirmer O F and Schnadt R 1976 Bound small polaron optical absorption in tetrahedral symmetry *Solid State Commun.* **18** 1345–8
[18] Dieke G H 1968 *Spectra and Energy Levels of Rare Earth Ions in Crystals* ed H M Crosswhite and H Crosswhite (New York: Interscience)
[19] Holgate S A, Sloane T H, Townsend P D, White D R and Chadwick A V 1994 Thermoluminescence of calcium fluoride doped with neodymium *J. Phys.: Condens. Matter* **6** 9255–66
[20] Hayes W and Stoneham A M 1985 *Defects and Defect Processes in Non-Metallic Solids* (New York: Wiley)
[21] Agullo-Lopez F, Catlow C R A and Townsend P D 1988 *Point Defects in Materials* (London: Academic)
[22] Song K S and William R T 1993 *Self Trapped Excitons* (Berlin: Springer)
[23] Karali T, Rowlands A P, Townsend P D, Prokic M and Olivares J 1998 Spectral comparison of Dy, Tm and Dy/Tm in $CaSO_4$ thermoluminescent dosimeters *J. Phys. D: Appl. Phys.* **31** 754–65
[24] Karali T, Townsend P D, Prokic M, and Rowlands A P 1999 Comparison of TL spectra of co-doped dosimetric materials *Radiat. Prot. Dosim.* **84** 281–4
[25] Nair B S K, Sundar D and Lakshmanan A R 2000 Thermostimulated luminescence and photoluminescence studies in $CaSO_4$:Ce; $CaSO_4$:Ce,Na; $CaSO_4$:Ce, Mn and $CaSO_4$:Ce, Mn, Na phosphors, at press
[26] Maghrabi M, Townsend P D and Lakshmanan A R 2000 Luminescence spectra of $CaSO_4$ with Ce, Dy, Mn and Ag codopants *J. Phys. D: Appl. Phys.* **33** 477–84
[27] Townsend P D and Rowlands A P 1999 Extended defect models for thermoluminescence *Radiat. Prot. Dosim.* **84** 7–12

[28] Karali T, Can N, Townsend P D, Rowlands A P and Hanchar J M 2000 Luminescence spectra of rare-earth element doped zircon *Am. Mineral.* at press
[29] Raymond S G, Luff B J, Townsend P D, Feng XiQi and Hu Guanquing 1994 Thermoluminescence spectra of doped $Bi_4Ge_3O_{12}$ *Radiat. Meas.* **23** 195–202
[30] Jazmati A K and Townsend P D 2000 Photoluminescence from RE doped BGO waveguides *Nucl. Instrum. Methods Phys. Res.* B at press
[31] Jazmati A K, Townsend P D and Vazquez G 2000 Second harmonic generation from RE doped BGO waveguides *Nucl. Instrum. Methods Phys. Res.* B at press
[32] *Handbook of Chemistry and Physics* 1972 ed R C Weast (Metals Park, OH: The Chemical Rubber Company)
[33] Townsend P D, unpublished